

Interconnection of $[V_{15}As_6O_{42}(H_2O)]^{6-}$ Clusters by Cu^{2+} -centered Complexes: Synthesis, Crystal Structure and Selected Properties

Adam Wutkowski^a, Christian Näther^a, Jan van Leusen^b, Paul Kögerler^b, and Wolfgang Bensch^a

^a Institut für Anorganische Chemie, Christian-Albrechts-Universität zu Kiel, Max-Eyth-Straße 2, D-24118 Kiel, Germany

^b Institut für Anorganische Chemie, RWTH Aachen, D-52074 Aachen, Germany

Reprint requests to Prof. W. Bensch. Phone: +49 431 880-2419. Fax: +49 431 880-1520.

E-mail: wbench@ac.uni-kiel.de

Z. Naturforsch. **2014**, *69b*, 1306–1314 / DOI: 10.5560/ZNB.2014-4161

Received July 25, 2014

Dedicated to Professor Hubert Schmidbaur on the occasion of his 80th birthday

The compound $\{[Cu(C_5H_{14}N_2)_2]_3[V_{15}As_6O_{42}(H_2O)]\}$ was synthesized under solvothermal conditions. During the reaction the V^V species of NH_4VO_3 are reduced to V^{IV} providing the 15 reduced V^{IV} centers in the anionic cluster. The compound crystallizes in the non-centrosymmetric orthorhombic space group $P2_12_12_1$ with four formula units in the cell, $V = 9464.8(4) \text{ \AA}^3$. The structure features $[V_{15}As_6O_{42}(H_2O)]^{6-}$ anions which are joined by Cu^{2+} -centered complexes to form linear chains. If a long Cu–O bond is considered as weak intermolecular interaction a three-dimensional network is generated. The compound is partially soluble in water as evidenced by UV/Vis spectroscopy and mass spectra. The magnetic susceptibility of the compound is dominated by strong intra-cluster anti-ferromagnetic exchange interactions.

Key words: Polyoxovanadate, Solvothermal Synthesis, Magnetic Properties, Crystal Structure

Introduction

The current interest and the intense research in the field of polyoxometalates (POMs) has very recently been summarized in several review articles [1–3]. According to these reviews the overwhelming research is focused on molybdenum- and tungsten-based POMs, and the potential of vanadium POM chemistry seems to be not exploited on a comparable level. Vanadium-based polyoxometalates have been studied by different working groups demonstrating the rich structural and electronic variability [4–13]. Moreover, vanadates and/or polyoxovanadates (POVs) have attracted high interest in the areas of supramolecular chemistry [14], as secondary electrode materials for advanced lithium batteries [15, 16] and as inorganic/organic hybrid materials for sorption applications [17]. In addition, reduced POVs were considered as promising materials in the field of catalysis as selective catalysts for the oxidation of *o*-xylene [18], and their catalytic properties have been studied [19, 20].

Of special interest are the magnetic properties of heterometal-substituted POVs like $K_6[V_{15}As_6O_{42}(H_2O)]$ [4–8] (abbreviated as $\{V_{15}\}$) which can be regarded as a prototype of a single molecule magnet. Up to now roughly 60 papers have reported on the properties of this compound (abbreviated as As-POV) with respect to butterfly hysteresis, loop of magnetization [21], antisymmetric exchange and Jahn-Teller effect [22], spin frustration [23, 24], and Rabi quantum oscillations [25], to mention just a few.

A chemical and physical modification of the $\{V_{15}\}$ cluster can be achieved by terminal expansion through a covalent linkage of transition metal complexes or organic molecules and by intracluster alteration either by generation of mixed-valent V centers or introduction of further heteroatoms [26–36]. Such modifications should lead to new exciting structure types, and it can also be expected that the physical properties of such modified clusters differ from those of the non-functionalized $\{V_{15}\}$ anion.

The Cambridge Structure Database (CSD) contains several arsenato POVs of general composition

$\{[Cu(\text{amine})_m][V_{18-x}As_{2x}O_{42}(Y)]\} \cdot nH_2O$ ($x = 2, 3, 4$; $Y = PO_4^{3-}, CO_3^{2-}, H_2O$). The majority of these compounds is based on the $[V_{14}As_8O_{42}(Y)]^{m-}$ ($Y = H_2O, CO_3^{2-}, PO_4^{3-}$) [30, 37–39] cluster type, and only a few feature the $[V_{15}As_6O_{42}(H_2O)]^{6-}$ $\{V_{15}\}$ shell. In the compound $\{[Cu(\text{en})_2]_{1.5}[H_3V_{15}As_6O_{42}(H_2O)]\} \cdot 3H_2O$ ($\text{en} = \text{ethylenediamine}$) [30] the $[Cu(\text{en})_2]^{2+}$ complex joins neighboring $\{V_{15}\}$ cluster anions by $V=O-Cu-O=V$ bridges leading to a sinusoidal chain structure. A chain is also observed in $[Co(\text{en})_3][\{Co(\text{en})_2\}_2V_{15}As_6O_{42}] \cdot 4H_2O$ [40] due to $Co-O_{\text{apical}}-V$ linkages with a $Co-O$ bond of 2.135 Å. A layered arrangement of the cluster anions is observed in the structure of $\{[Cu(\text{enMe})_2]_{2.5}[HAs_6V_{15}O_{42}(H_2O)]\} \cdot 2H_2O$ ($\text{enMe} = 1,2$ diaminopropane) *via* $Cu-O_{\text{apical}}-V$ bridges [41]. Linear chains are built in $\{[Ni(\text{en})_2]V_{15}As_6O_{42}(H_2O)]^{4-}$ by $Ni-O_{\text{apical}}-V$ linkages, while a helical chain is found in the structure of $[Zn_2(\text{dien})_3(H_2O)_2]_{1/2}[\{Zn_2(\text{dien})_3\}V_{15}As_6O_{42}(H_2O)] \cdot 2H_2O$ [29]. In the compound $[Co(\text{enMe})_2]_3[V_{15}As_6O_{42}(H_2O)] \cdot 2H_2O$ the cluster anion is surrounded by six Co^{2+} -centered complexes, and a layer is formed [29]. In the two compounds $[Zn(\text{en})_2][Zn(\text{en})_2(H_2O)_2][\{Zn(\text{en})(\text{enMe})\}V_{15}As_6O_{42}(H_2O)] \cdot 4H_2O$ and $[Zn_2(\text{enMe})_2(\text{en})_3][\{Zn(\text{enMe})_2\}V_{15}As_6O_{42}(H_2O)] \cdot 4H_2O$ the spherical clusters are expanded by one Zn^{2+} -centered complex [42]. These examples demonstrate the structural versatility of As -POVs chemically modified by transition metal complexes.

During our research in the area of POVs and chemically modified POVs we recently isolated several new polyoxovanadates under hydrothermal conditions [43–59]. All these compounds were synthesized applying NH_4VO_3 as a V source, and the amines used in the syntheses act as reducing agents to reduce V^V to V^{IV} . We now extended the synthetic work to arsenato POVs, and in this contribution we present the new compound $\{[Cu(C_5H_{14}N_2)_2]_3[V_{15}As_6O_{42}(H_2O)]\}$ featuring a 3D network constructed by interconnection of the $\{V_{15}As_6\}$ clusters by Cu^{2+} -centered complexes.

Experimental Part

Synthesis

The compound was prepared under solvothermal conditions in 15 mL glass tubes with Duran PBT screw caps (GL18). A mixture of $CuCl_2 \cdot 2 H_2O$ (150 mg,

0.85 mmol), NH_4VO_3 (200 mg, 1.7 mmol), As_2O_3 (150 mg, 0.75 mmol), 2,2-dimethylpropyldiamine (2 mL), and H_2O (2 mL) ($pH = 10.8$ at $19^\circ C$) was heated at $150^\circ C$ for seven days. After this time, the tube was allowed to cool down. The reaction product was collected by filtration and washed with water and ethanol. The compound was obtained as dark-green plates, and the yield based on vanadium was about 78%. Elemental analysis found C 14.83, H 3.70, N 6.90%; calcd. C 13.30; H 3.20; N 6.21%. The differences between experimentally determined and calculated values may be traced back to the presence of solvent molecules which could not be located during crystal structure determination.

Mass spectroscopy

Mass spectra were collected on an Applied Biosystem Mariner 5280 mass spectrometer in electrospray ionization (ESI) mode (positive ion scan mode).

Thermal analysis

The TG measurements were conducted with a heating rate of $4 K \text{ min}^{-1}$ in Al_2O_3 crucibles in a dynamic helium atmosphere with a flow-rate of 75 mL min^{-1} using a STA-409CD device (Netzsch). The TG data were corrected for buoyancy and current effects.

Infrared spectroscopy

IR spectra (400 to 4000 cm^{-1}) of the title compound were recorded with a Nicolet Avatar 360 FT-IR ESP spectrometer using KBr pellets.

UV/Vis spectroscopy

UV/Vis spectroscopy investigations were conducted at room temperature using a UV/Vis two-channel spectrometer Cary 5 from Varian Techtron Pty., Darmstadt.

Elemental analysis

Elemental analyses were obtained using a EURO EA Elemental Analyzer, fabricated by EURO VECTOR Instruments and Software.

Single-crystal structure analysis

Data collection was performed using an imaging plate diffraction system (IPDS-2 with $MoK\alpha$ radiation from Stoe & Cie. The data were corrected for absorption using X-RED and X-SHAPE from Stoe. Structure solution was performed with Direct Methods using SHELXS-97, and structure refinements were performed against F^2 using SHELXL-97 [60]. Most non-hydrogen atoms were refined with anisotropic displacement parameters. The hydrogen atoms were positioned with idealized geometry and were refined with $U_{\text{iso}}(H) = -1.2 U_{\text{eq}}(C, N)$ (1.5 for methyl H atoms) using a riding model. Within the cluster anion a water molecule is located

for which the O–H H atoms were not located but considered in the molecular formula. For some of the C and N atoms of the ligands too high anisotropic displacement parameters were found, indicating for large structural disorder. Refinement using a split model did not lead to any significant improvement of the structure model. Therefore, these atoms were refined only isotropically. After the final refinement several electron density peaks were found indicating disordered water or ligand molecules, for which no reasonable split model could be found. Therefore, the data were corrected for disordered solvent molecules using the SQUEEZE option in PLATON [61]. The relatively high reliability factors can be traced back to the poor crystal quality. Reciprocal space plots reveal that the investigated crystal contained small contributions of additional individuals that could not be indexed separately. Several data sets were measured for different crystals even at lower temperatures but no better data sets were obtained. Details of the structure determination are given in Table 1.

CCDC 1024091 contains the supplementary crystallographic data for this paper. These data can be obtained free of charge from The Cambridge Crystallographic Data Centre via www.ccdc.cam.ac.uk/data_request/cif.

Magnetic measurements

Magnetic measurements were performed between 2 and 290 K using a Quantum Design MPMS-5XL SQUID magnetometer. The sample was compacted and immobilized into a cylindrical PTFE capsule. The data were corrected for contributions of the sample holder and the diamagnetic contribution ($\chi_{\text{m,dia}} = -1.14 \times 10^{-3} \text{ cm}^3 \text{ mol}^{-1}$).

Results and Discussion

Compound **1** crystallizes in the non-centrosymmetric orthorhombic space group $P2_12_12_1$ with $Z = 4$ and all unique atoms located on general positions (Table 1).

The $[\text{V}_{15}\text{As}_6\text{O}_{42}(\text{H}_2\text{O})]^{6-}$ cluster anion consists of 15 distorted $\{\text{VO}_5\}$ square pyramids that are interlinked through the basal O vertices and edges and of six $\{\text{AsO}_3\}$ trigonal pyramids. ($\text{V}-(\mu\text{-O})$: 1.892(11)–2.087(11) Å, $\text{V}=\text{O}_{\text{term}}$: 1.576(11)–1.632(13) Å). The structural motif can be derived from the $[\text{V}_{18}\text{O}_{42}]^{12-}$ archetype structure by substitution of three $\{\text{VO}_5\}$ pyramids by three handle-like $\{\text{As}_2\text{O}_5\}$ dimers ($\text{As}-\text{O}$: 1.717(11)–1.810(12) Å) centered around the equatorial plane of the cluster. In the center of the cluster a water molecule is encapsulated. An alternative description of the structure is based on VO_5 pyramids which are condensed to

Table 1. Selected crystal data and details of the structure determination for the title compound.

Empirical formula	$\text{C}_{30}\text{H}_{86}\text{As}_6\text{Cu}_3\text{N}_{12}\text{O}_{43}\text{V}_{15}$
M_r , g mol^{-1}	2707.35
Crystal system	orthorhombic
Space group	$P2_12_12_1$
a , Å	12.2124(3)
b , Å	25.4444(6)
c , Å	30.4591(8)
V , Å ³	9464.8(4)
T , K	293
Z	4
$D_{\text{calcd.}}$, mg cm^{-3}	1.90
μ , mm^{-1}	4.2
θ_{max} , deg	1.6–24.7
Measured reflections	65 950
Unique reflections	15 913
R_{int}	0.1271
Min/max transmission	0.4644/0.6213
Refl. with $F_o > 4 \sigma(F_o)$	12 661
Parameters	878
R_1^a [$F_o > 4 \sigma(F_o)$]	0.0902
wR_2^b (all data)	0.2057
GoF ^c	1.081
$\Delta\rho_{\text{max/min}}$ $e \text{ Å}^{-3}$	0.68/−0.71

^a $R_1 = \Sigma||F_o| - |F_c||/\Sigma|F_o|$; ^b $wR_2 = [\Sigma w(F_o^2 - F_c^2)^2/\Sigma w(F_o^2)^2]^{1/2}$, $w = [\sigma^2(F_o^2) + (AP)^2 + BP]^{-1}$, where $P = (\text{Max}(F_o^2, 0) + 2F_c^2)/3$; ^c $\text{GoF} = [\Sigma w(F_o^2 - F_c^2)^2/(n_{\text{obs}} - n_{\text{param}})]^{1/2}$.

form two V_6 hexagons and one V_3 triangle being unwrapped by the hexagons.

Considering only Cu–O distances below 3.0 Å the cluster anion is expanded by four $[\text{Cu}(\text{C}_6\text{H}_{14}\text{N}_2)_2]^{2+}$ complexes. Two Cu^{2+} ions (Cu1, Cu2) are surrounded by four N atoms of two bidentate amine ligands and one terminal O^{2-} ion of the cluster anion (see Fig. 1). The resulting CuN_4O polyhedra may be described as a distorted rectangular pyramid. The Cu(1,2)–N (1.985(16)–2.045(15) Å) as well as the Cu(1,2)–O (2.292(9) and 2.236(10) Å) bond lengths are in the range reported for Cu–N/O complexes [30, 34, 37–39]. The third unique Cu^{2+} cation, Cu(3), is in a distorted octahedral environment of four N atoms of two ligands and of two terminal O atoms of the cluster anion (Cu(3)–N: 1.98(2)–2.05(3) Å; Cu(3)–O: 2.284(12) and 2.521(12) Å). For polyoxovanadates and As-POVs the Cu–O bonds vary between about 2.0 and 2.7 Å depending on the geometry around Cu and the type of oxygen atom of the vanadate anion. *E.g.*, the Cu^{2+} center in an octahedral environment in $\{[(\text{CuL})_{0.5}(\text{H}_2\text{L})_{1.5}][\text{H}_2\text{V}_{10}\text{O}_{28}] \cdot 6\text{H}_2\text{O}\}_n$ ($L = 5,5,7,12,12,14$ -hexamethyl-1,4,8,11-tetraazacy-

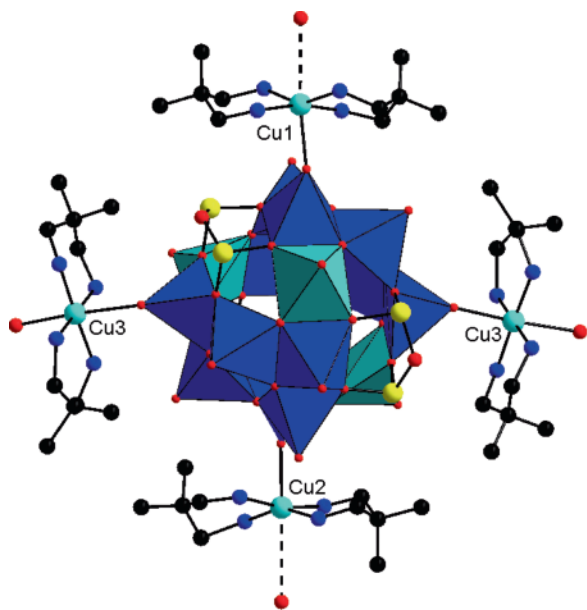


Fig. 1 (color online). The structure of the $\{[Cu(C_6H_{14}N_2)_2]_3[V_{15}As_6O_{42}(H_2O)]\}$ cluster in the crystal. The VO_5 polyhedra belonging to the V_6 hexagon are shown in dark blue, and the three central VO_5 groups are drawn in turquoise. The long Cu–O separations are shown as dashed lines. H atoms are omitted for clarity.

clotradecane) shows a Cu–O bond of 2.525(3) Å [62], while two different distances (2.448(4) and 2.451(4) Å) are observed in $(Hpz)_2\{[Cu(pz)_4]_2V_{10}O_{28}\} \cdot 2H_2O$ (pz = pyrazole) [63]. An even longer Cu–O bond of 2.665(2) Å was found in the structure of $[Cu(2-amp)_2(H_2O)]_2H_2V_{10}O_{28} \cdot 4H_2O$ (amp = 2-(aminomethyl)pyridine) [64]. For a decavanadate with a Cu center in a *tetragonal-pyramidal* environment the Cu–O bond length is significantly shorter at 2.1524(18) Å in $(NH_4)_2[Cu_2(NH_3CH_2CH_2COO)_4(V_{10}O_{28})] \cdot 10H_2O$ [65]. The compound $\{Cu(pz)_4\}_4\{[Cu(pz)_3]_2V_{10}O_{28}\}$ features a Cu atom with a *trigonal-bipyramidal* coordination geometry, and the Cu–O bonds are very different at 1.962(2) and 2.313(2) Å [63].

The $Cu(2)^{2+}$ cation has a next nearest O atom at 3.3390(11) Å, a distance too long for a significant bonding interaction, while the $Cu(1)^{2+}$ ion has an O atom of a neighboring cluster anion at 3.022(12) Å, thus enhancing the coordination number to 5 + 1. These long Cu–O separations are caused by the Jahn-Teller effect of the $Cu^{2+} d^9$ electronic configuration and are frequently observed in such

compounds. Taking only the Cu–O bonds below 3 Å into account a chain along [001] is generated with alternating $Cu(3)^{2+}$ -centered complex cations and $[V_{15}As_6O_{42}(H_2O)]^{6-}$ anions (Fig. 2). Considering the Cu–O distance of 3.022(12) Å as a weak bond, these chains are joined to form a three-dimensional network. The connection pattern generates blocks consisting of six interconnected cluster anions within the (100) plane. Along [010] the clusters alternate in an $\cdots A-B-A \cdots$ fashion, and the interconnection of the cluster shells by the Cu(1)-centered complexes along [010] leads to the formation of zig-zag chains (Fig. 2, bottom).

As mentioned in the introduction some As-POV clusters interconnected by TM complexes have been reported in the past. Concerning those containing Cu-centered complexes different dimensionalities have been observed. In the compound $\{[Cu(enMe)_2]_{2.5}[HAS_6V_{15}O_{42}(H_2O)]\} \cdot 2H_2O$ [41] the anionic $[HAS_6V_{15}O_{42}(H_2O)]^{5-}$ clusters are interconnected by Cu^{2+} -centered complexes acting as two double-bridges generating linear chains. The chains are further joined by another Cu^{2+} complex yielding a layer structure. The Cu–O_{term} bonds are between 2.398(5) and 2.670(6) Å. In the second compound featuring Cu^{2+} and the $\{V_{15}As_6\}$ cluster, $[Cu(en)_2]_{1.5}[H_3As_6V_{15}O_{42}(H_2O)] \cdot 3H_2O$ [30], a sinusoidal chain structure is observed by interconnection of the anions by two unique Cu^{2+} cations each being in an octahedral environment. Three terminal oxygen atoms of VO_5 pyramids of the cluster are involved in the Cu–O bonding with Cu–O bond lengths between 2.271(9) and 2.74(6) Å.

Bond valence calculation (BVS) [66] of the As atoms in the title compound indicate an oxidation state close to 3 with values ranging from 3.04 to 3.279. For the 15 independent V centers the BVS values are between 3.975 and 4.258 (average: 4.141, Table 2). A short comparison with BVS data reported in the literature is necessary in order to classify those calculated for the title compound. For the $\{V_{18}\}$ cluster several mixed-valent states are well known. According to ref. [4] for a $V^{IV}_{16}V^V_2O_{42}$ -type cluster with non-localized V^{IV} centers a BVS value between 4.24 and 4.37 is expected, while the average value for a fully reduced cluster is between 4.07 and 4.23. For $(NH_4)_8[V_{18}O_{42}(SO_4)] \cdot 25H_2O$ the assignment of oxidation states according to $\{V^{IV}_{12}V^V_6\}$ corresponds to an average BVS value of 4.37 per vanadium cen-

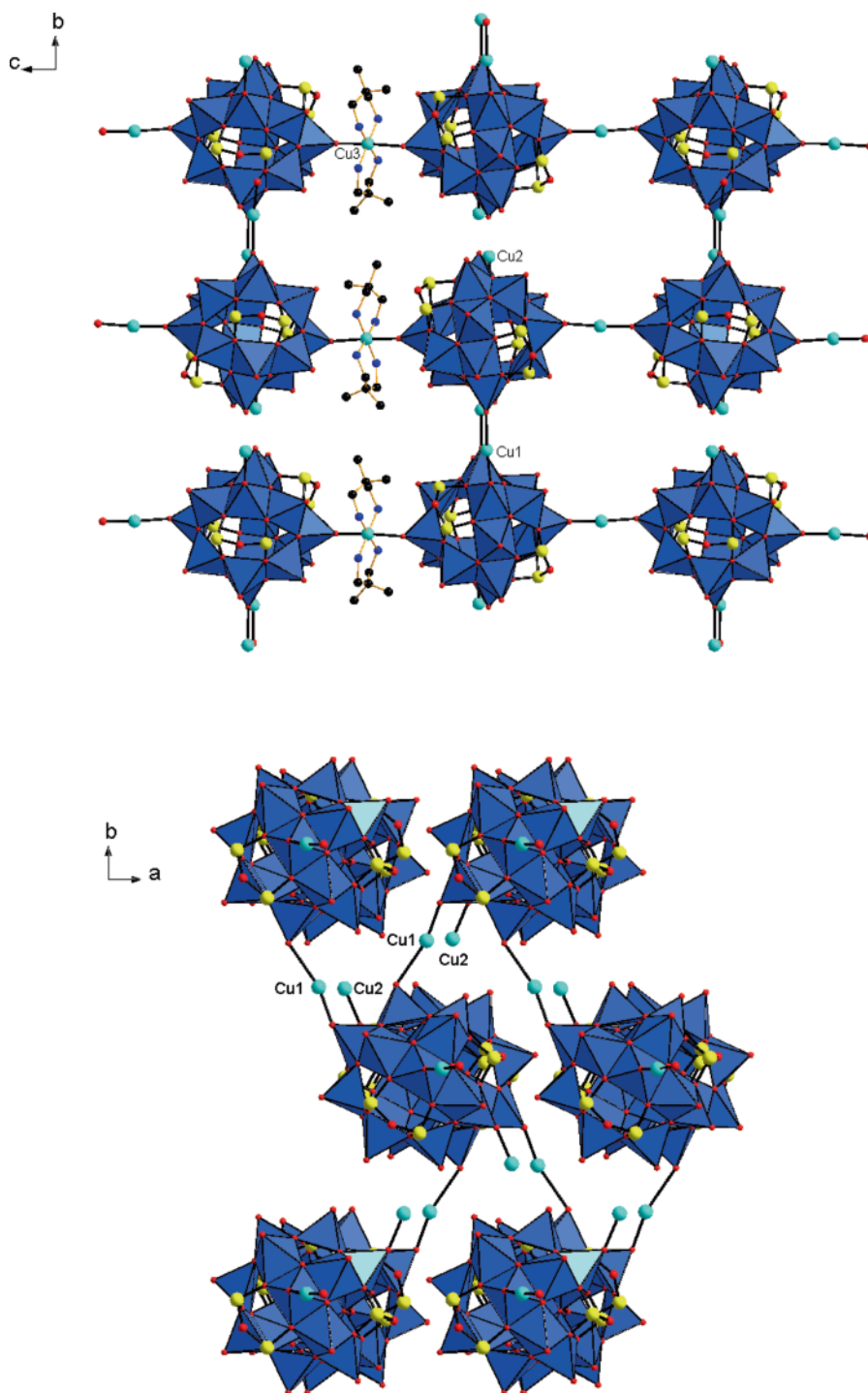


Fig. 2 (color online). Arrangement of $\{[\text{Cu}(\text{C}_6\text{H}_{14}\text{N}_2)_2]_3[\text{V}_{15}\text{As}_6\text{O}_{42}(\text{H}_2\text{O})]\}$ in a 3D network achieved by linking of the $[\text{V}_{15}\text{As}_6\text{O}_{42}(\text{H}_2\text{O})]^{6-}$ clusters with $[\text{Cu}(\text{C}_6\text{H}_{14}\text{N}_2)_2]^{2+}$ complexes. Top: view along [100]; bottom: view along [001]. Only some of the ligands are displayed.

Table 2. Calculated bond valence values for the title compound. The last column gives the deviation from the oxidation state 4+ in %.

Atom	BVS	Deviation (%)
V1	4.258	6
V2	4.191	5
V3	4.081	2
V4	4.181	5
V5	4.194	5
V6	4.018	0
V7	4.197	5
V8	4.115	3
V9	4.092	2
V10	4.239	6
V11	3.975	1
V12	4.163	4
V13	4.245	6
V14	4.048	1
V15	4.119	3

ter [5]. These examples demonstrate that the average BVS value calculated for the cluster anion of the title compound points towards V^{IV} centers.

The calculation of bond valence sums for Cu^{2+} in a Jahn-Teller-distorted environment is not straightforward because no unique R_0 value is available. Due to the fact that the three independent Cu atoms exhibit a strongly distorted coordination environment the presence of Cu^+ can be excluded.

In the IR spectrum (see Fig. 3) the characteristic terminal $\nu_s(\text{V}=\text{O})$ vibration is located at 981 cm^{-1} which is typical for $\text{V}^{\text{IV}}=\text{O}$. The IR spectrum also contains the characteristic vibrations of organic molecules and of water.

The compound could be partially dissolved in H_2O , and the UV/Vis difference spectrum of the solution shows an absorption maximum at 200 nm and a shoulder at 260 nm (Fig. 4).

The powder X-ray pattern of the residue not dissolved in H_2O displays no changes compared to the diffractogram of the pristine material. In the IR spectrum of the residue, the characteristic $\text{V}=\text{O}$ band occurs at the same positions as for **1**. According to EDX analysis a change in the $\text{Cu}:\text{V}:\text{As}$ ratio is detected after treatment with H_2O ($\text{Cu}:\text{V}:\text{As} = 1:1.25:1.32$; original: $1:2.26:1.58$), and it seems that some of the Cu complexes were removed from the pristine material. The ESI-MS spectrum of the solution (Fig. 5) is complex, and an interpretation is not straightforward due to the formation of clusters with attached solvent molecules, aggregation, or conversion into other

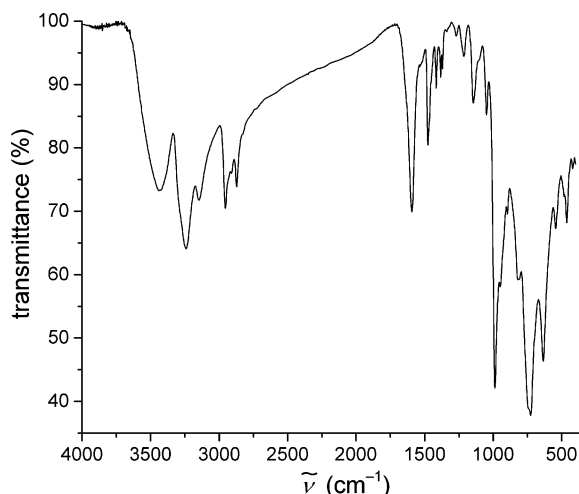


Fig. 3. IR spectrum of the title compound.

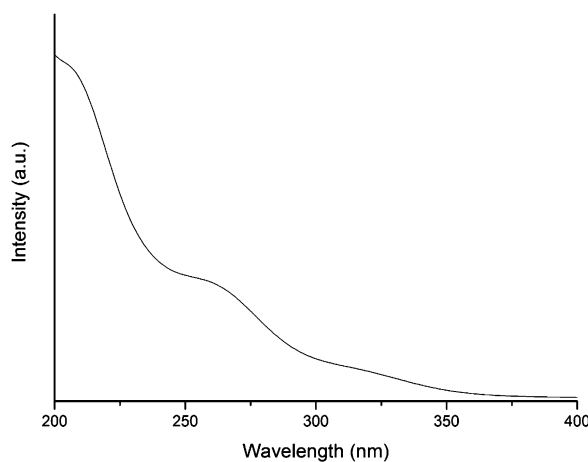


Fig. 4. UV/Vis difference spectrum of the solution of the title compound in H_2O .

species [67]. The two most prominent mass peaks are at $m/z = 413$ and 659 . Despite many trials an unambiguous assignment of the two peaks to a distinct cluster could not be obtained. In any case, UV/Vis and MS spectra give evidences that the title compound is at least partially soluble in H_2O .

The material dissolved in H_2O was recovered by removal of the solvent. The powder pattern of this product is characterized by strong modulation of the background which is typical of amorphous substances.

In the TG curve of the title compound (Fig. 6) a slight mass loss occurs between about 100 and $200\text{ }^\circ\text{C}$ which may be attributed to the release of wa-

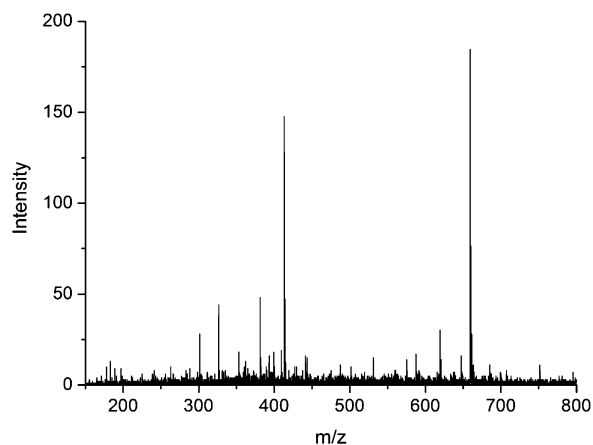


Fig. 5. Mass spectrum of the water solution of the title compound.

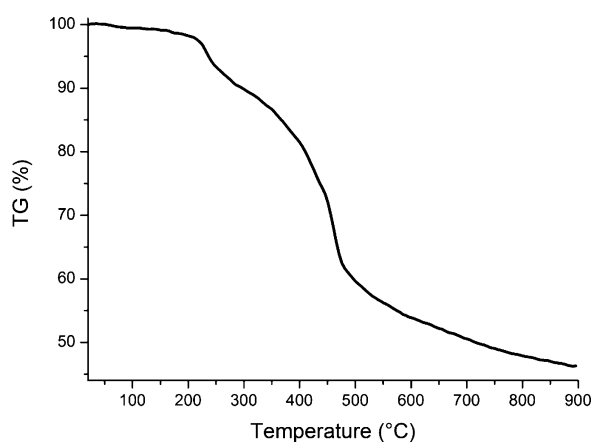


Fig. 6. TGA curve of the title compound.

ter. Above 200 °C a not well-resolved mass loss step (*ca.* 10%) is observed followed by a mass decrease of about 30% up to 480 °C. Above this temperature further volatile species are released, and at 900 °C the weight change is still not finished.

The magnetic susceptibility data of $\{[\text{Cu}(\text{C}_6\text{H}_{14}\text{N}_2)_2]_3[\text{V}_{15}\text{As}_6\text{O}_{42}(\text{H}_2\text{O})]\}$ are presented as the product $\chi_m T$ *vs.* T in Fig. 7 (experimental values: blue open circles). The interpretation of the magnetic data of transition metal-supported polyoxovanadate(IV) clusters often has to account for significantly different exchange interactions. In the title compound, the spin core structure of the $[\text{V}_{15}\text{As}_6\text{O}_{42}(\text{H}_2\text{O})]^{6-}$ cluster anion is characterized by all-antiferromagnetic intra-cluster coupling that is very strong in the

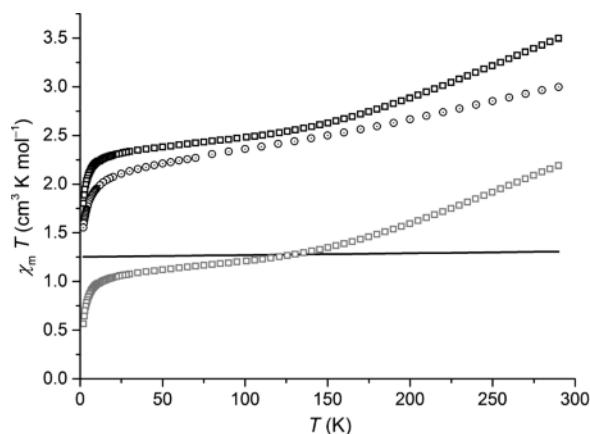


Fig. 7. Temperature dependence of the product $\chi_m T$ at $B = 0.1$ Tesla; experimental data of $\{[\text{Cu}(\text{C}_6\text{H}_{14}\text{N}_2)_2]_3[\text{V}_{15}\text{As}_6\text{O}_{42}(\text{H}_2\text{O})]\}$ (open circles) and of $\text{K}_6[\text{V}_{15}\text{As}_6\text{O}_{42}(\text{H}_2\text{O})]$ (squares) [4–8], calculated single-ion contributions of three non-interacting Cu^{2+} centers in Jahn–Teller-distorted octahedral ligand fields (straight line) and, for comparison, the sum of cluster anion and Cu^{2+} contributions (line + squares).

outer two V_6 rings and weak between the three vanadyl groups situated in the equatorial plane of the cluster, resulting in geometric frustration of the spin-1/2 centers. The susceptibility of an individual $\{\text{V}_{15}\text{As}_6\}$ cluster is shown as open squares in Fig. 7. Note that the antiferromagnetic coupling results in a value of $\chi_m T = 2.19 \text{ cm}^3 \text{ mol}^{-1}$ at 290 K that is well below $5.40 \text{ cm}^3 \text{ mol}^{-1}$, the theoretical value of 15 non-interacting V^{4+} centers, assuming $\chi_m T \approx 0.36 \text{ cm}^3 \text{ mol}^{-1}$ per center.

Simulated single-ion contributions of three Cu^{2+} (spin-1/2) centers in tetragonally elongated (*i. e.* Jahn–Teller-distorted) coordination environments are shown as straight line in Fig. 7 to estimate the impact of the bridging Cu^{2+} centers, assuming a strongly distorted ligand field of D_{4h} or C_{4v} symmetry. The sum of the $\chi_m T$ data of the $[\text{V}_{15}\text{As}_6\text{O}_{42}(\text{H}_2\text{O})]^{6-}$ cluster anion and the Cu^{2+} centers leads to the straight line and squares combination which deviates from the experimental data of $\{[\text{Cu}(\text{C}_6\text{H}_{14}\text{N}_2)_2]_3[\text{V}_{15}\text{As}_6\text{O}_{42}(\text{H}_2\text{O})]\}$, yielding slightly higher $\chi_m T$ values; the absolute deviation averaged over the entire 2–290 K measurement interval amounts to $0.23 \text{ cm}^3 \text{ K mol}^{-1}$. We note that these deviations are larger than for previously reported transition metal-substituted $\{\text{V}_{15}\text{E}_6\}$ -type compounds, where the experimental susceptibility is well repro-

duced by the sum of the contributions of the polyoxovanadate core and the transition metal constituents. We tentatively link these deviations to (weak) antiferromagnetic exchange interactions between the $\{V_{15}As_6\}$

cluster cores and the adjoined Cu(II) centers, as well as to higher exchange energies within the $\{V_{15}As_6\}$ cores that would mostly affect the high-temperature region of the susceptibility data.

- [1] D.-L. Long, R. Tsunashima, L. Cronin, *Angew. Chem. Int. Ed.* **2010**, *49*, 1736–1758.
- [2] A. Dolbecq, C. R. Mayer, P. Mialane, *Chem. Rev.* **2010**, *110*, 6009–6048.
- [3] U. Kortz, A. Müller, J. van Slageren, J. Schnack, N. S. Dalal, M. Dressel, *Coord. Chem. Rev.* **2009**, *253*, 2315–2327.
- [4] A. Müller, R. Sessoli, E. Krickemeyer, H. Bögge, J. Meyer, D. Gatteschi, L. Pardi, J. Westphal, K. Hove-meier, R. Rohlfing, J. Döring, F. Hellweg, C. Beugholt, M. Schmidtmann, *Inorg. Chem.* **1997**, *36*, 5239–5250.
- [5] A. Müller, J. Döring, *Z. Anorg. Allg. Chem.* **1991**, *595*, 251–274.
- [6] M. T. Pope, A. Müller, *Angew. Chem., Int. Ed. Engl.* **1991**, *30*, 34–48.
- [7] A. Müller, J. Döring, *Angew. Chem., Int. Ed. Engl.* **1988**, *27*, 1721.
- [8] D.-L. Long, D. Orr, G. Seeber, P. Kögerler, L. J. Farrugia, L. Cronin, *J. Cluster Sci.* **2003**, *14*, 313–324.
- [9] M. T. Pope, A. Müller (Eds.), *Polyoxometalates: From Platonic Solids to Anti-Retroviral Activity*, Kluwer Academic Publishers, Dordrecht **1994**.
- [10] M. T. Pope, A. Müller (Eds.), *Polyoxometalate chemistry: From Topology via Self-Assembly to Applications*, Kluwer Academic Publishers, Dordrecht, **2001**.
- [11] G. Huan, M. A. Greaney, A. J. Jacobson, *J. Chem. Soc., Chem. Commun.* **1991**, 260–261.
- [12] X.-B. Cui, K.-C. Li, L. Ye, Y. Chen, J.-Q. Xu, W.-J. Duan, H.-H. Yu, Z.-H. Yi, J.-W. Cui, *J. Solid State Chem.* **2008**, *181*, 221–227.
- [13] M. Khan, Q. Chen, J. Zubieta, *Inorg. Chim. Acta* **1993**, *212*, 199–206.
- [14] A. Müller, H. Reuter, S. Dillinger, *Angew. Chem., Int. Ed. Engl.* **1995**, *34*, 2328–2361.
- [15] M. S. Whittingham, *J. Electrochem. Soc.* **1976**, *123*, 315–320.
- [16] T. A. Chirayli, P. Y. Zavalij, M. S. Whittingham, *J. Electrochem. Soc.* **1996**, *143*, L193–L195.
- [17] J. Do, A. J. Jacobson, *Inorg. Chem.* **2001**, *40*, 2468–2469.
- [18] J. Spengler, F. Anderle, E. Bosch, R. K. Grasselli, B. Pillep, P. Behrens, O. B. Lapina, A. A. Shubin, H.-J. Eberle, H. J. Knözinger, *J. Phys. Chem. B* **2001**, *105*, 10772–10783.
- [19] M. I. Khan, S. Tabussum, C. L. Marshall, M. K. Neylon, *Catal. Lett.* **2006**, *112*, 1–12.
- [20] M. I. Khan, K. Aydemir, M. R. H. Siddiqui, A. A. Alwarthan, C. L. Marshall, *Catal. Lett.* **2011**, *141*, 538–543.
- [21] I. Chiorescu, W. Wernsdorfer, A. Müller, S. Miyashita, B. Barbara, *Phys. Rev. B: Condens. Matter* **2003**, *67*, 020402.
- [22] D. A. Tarantul, B. Tsukerblat, A. Müller, *Inorg. Chem.* **2007**, *46*, 161–169.
- [23] G. Chaboussant, S. T. Ochsenein, A. Sieber, H.-U. Güdel, H. Mutka, A. Müller, B. Barbara, *Europhys. Lett.* **2004**, *66*, 423–429.
- [24] G. Chaboussant, R. Basler, A. Sieber, S. T. Ochsenein, A. Desmedt, R. E. Lechner, M. T. F. Telling, P. Kögerler, A. Müller, H.-U. Güdel, *Europhys. Lett.* **2002**, *59*, 291–297.
- [25] S. Bertaina, S. Gambarelli, T. Mitra, B. Tsukerblat, A. Müller, B. Barbara, *Nature* **2008**, *453*, 203–206.
- [26] S.-T. Zheng, J. Zhang, G.-Y. Yang, *J. Mol. Struct.* **2005**, *752*, 25–31.
- [27] X.-B. Cui, J.-Q. Xu, L. Ding, H. Ding, L. Ye, G.-Y. Yang, *J. Mol. Struct.* **2003**, *660*, 131–137.
- [28] Y. Qi, Y. Li, E. Wang, H. Jin, Z. Zhang, X. Wang, S. Chang, *J. Solid State Chem.* **2007**, *180*, 382–389.
- [29] S.-T. Zheng, Y.-M. Chen, J. Zhang, J.-Q. Xu, G.-Y. Yang, *Eur. J. Inorg. Chem.* **2006**, 397–406.
- [30] X.-B. Cui, J.-Q. Xu, Y.-H. Sun, Y. Li, L. Ye, G.-Y. Yang, *Inorg. Chem. Commun.* **2004**, *7*, 58–61.
- [31] S.-T. Zheng, J. Zhang, B. Li, G.-Y. Yang, *Dalton Trans.* **2008**, 5584–5587.
- [32] S.-T. Zheng, J. Zhang, J.-Q. Xu, G.-Y. Yang, *J. Solid State Chem.* **2005**, *178*, 3740–3746.
- [33] X.-B. Cui, J.-Q. Xu, Y. Li, Y.-H. Sun, G.-J. Yang, *Eur. J. Inorg. Chem.* **2004**, 1051–1055.
- [34] X.-B. Cui, J.-Q. Sun, G.-Y. Yang, *Inorg. Chem. Commun.* **2003**, *6*, 259–261.
- [35] T. Arumuganathan, S. K. Das, *Inorg. Chem.* **2009**, *48*, 496–507.
- [36] B.-X. Dong, J. Peng, C. J. Gomez-Garcia, S. Benmansour, H.-Q. Jia, N.-H. Hu, *Inorg. Chem.* **2007**, *46*, 5933–5941.
- [37] Y.-F. Li, L.-M. Zhang, C.-L. Liu, F. Zhang, J. Zou, J.-X. Sun, Y. Bai, Y.-Q. Sun, Y. Tian, *Chem. J. Chin. Univ. (Chinese Edition)* **2006**, *27*, 2260–2262.
- [38] B.-X. Dong, P.-P. Zhang, J. Peng, *Chem. J. Chin. Univ. (Chinese Edition)* **2007**, *28*, 1018–1020.

- [39] Y.-F. Qi, Y.-G. Li, E. Wang, D.-R. Xiao, J. Hua, *J. Coord. Chem.* **2007**, *60*, 1403–1408.
- [40] W.-M. Bu, G.-Y. Yang, L. Ye, J.-Q. Xu, Y.-G. Fan, *Chem. Lett.* **2000**, 462–463.
- [41] S.-Y. Shi, Y. Chen, J.-N. Xu, Y.-C. Zou, X.-B. Cui, Y. Wang, T.-G. Wang, J.-Q. Xu, Z.-M. Gao, *CrystEngComm* **2010**, *12*, 1949–1954.
- [42] S.-T. Zheng, Y.-M. Chen, J. Zhang, G.-Y. Yang, *Z. Anorg. Allg. Chem.* **2006**, *632*, 155–159.
- [43] J. Wang, C. Näther, M. Speldrich, P. Kögerler, W. Bensch, *CrystEngComm* **2013**, *15*, 10238–10245.
- [44] A. Wutkowski, C. Näther, P. Kögerler, W. Bensch, *Inorg. Chem.* **2013**, *52*, 3280–3284.
- [45] E. Antonova, C. Näther, W. Bensch, *CrystEngComm* **2012**, *14*, 6853–6859.
- [46] E. Antonova, C. Näther, P. Kögerler, W. Bensch, *Dalton Trans.* **2012**, *41*, 6957–6962.
- [47] J. Wang, C. Näther, P. Kögerler, W. Bensch, *Eur. J. Inorg. Chem.* **2012**, 1237–1242.
- [48] E. Antonova, C. Näther, P. Kögerler, W. Bensch, *Inorg. Chem.* **2012**, *51*, 2311–2317.
- [49] E. Antonova, C. Näther, W. Bensch, *Dalton Trans.* **2012**, *41*, 1338–1344.
- [50] E. Antonova, A. Wutkowski, C. Näther, W. Bensch, *Solid State Sci.* **2011**, *13*, 2154–2159.
- [51] A. Wutkowski, F. Niefind, C. Näther, W. Bensch, *Z. Anorg. Allg. Chem.* **2011**, *637*, 2198–2204.
- [52] A. Wutkowski, N. Evers, W. Bensch, *Z. Anorg. Allg. Chem.* **2011**, *637*, 2205–2210.
- [53] E. Antonova, P. Kögerler, C. Näther, W. Bensch, *Angew. Chem. Int. Ed.* **2011**, *50*, 764–767.
- [54] J. Wang, C. Näther, P. Kögerler, W. Bensch, *Inorg. Chim. Acta* **2010**, *363*, 4399–4404.
- [55] A. Wutkowski, C. Näther, M. Speldrich, P. Kögerler, W. Bensch, *Z. Anorg. Allg. Chem.* **2009**, *635*, 1094–1099.
- [56] A. Wutkowski, C. Näther, P. Kögerler, W. Bensch, *Inorg. Chem.* **2008**, *47*, 1916–1918.
- [57] R. Kiebach, C. Näther, P. Kögerler, W. Bensch, *Dalton Trans.* **2007**, 3221–3223.
- [58] R. Kiebach, C. Näther, W. Bensch, *Solid State Sci.* **2006**, *8*, 964–970.
- [59] D. Pitzschke, J. Wang, R.-D. Hoffmann, R. Pöttgen, W. Bensch, *Angew. Chem. Int. Ed.* **2006**, *45*, 1305–1308.
- [60] G. M. Sheldrick, *Acta Crystallogr.* **2008**, *A64*, 112–122.
- [61] A. L. Spek, *Acta Crystallogr.* **2009**, *D65*, 148–155.
- [62] Y. Qi, E. Wang, J. Li, Y. Li, *J. Solid State Chem.* **2009**, *182*, 2640–2645.
- [63] J. Thomas, M. Agarwal, A. Ramanan, N. Chernova, M. S. Whittingham, *CrystEngComm* **2009**, *11*, 625–631.
- [64] L. Bartošová, Z. Padelková, E. Rakovsky, P. Schwendt, *Polyhedron* **2012**, *31*, 565–569.
- [65] L. Klištincová, E. Rakovsky, P. Schwendt, *Inorg. Chem. Commun.* **2008**, *11*, 1140–1142.
- [66] Bond valence sums were determined using the software VALIST by A. S. Wills, Program available from www.ccp14.ac.uk.
- [67] D.-L. Long, C. Streb, Y.-F. Song, S. Mitchell, L. Cronin, *J. Am. Chem. Soc.* **2008**, *130*, 1830–1832.